



Effects of electric pulse heat treatment on microstructures and dynamic deformation behaviors of Ti6441 alloys

Dongmei Huo^{a,b}, Shukui Li^{a,b}, Qunbo Fan^{a,b,*}, Fuchi Wang^{a,b}

^a School of Materials Science and Engineering, Beijing Institute of Technology, Beijing 100081, China

^b National Key Laboratory of Science and Technology on Materials Under Shock and Impact, Beijing 100081, China

ARTICLE INFO

Article history:

Received 27 July 2011

Received in revised form

14 September 2011

Accepted 15 September 2011

Available online 21 September 2011

Keywords:

Titanium alloy

Electric pulse heat treatment

Microstructure

Mechanical characterization

Shear bands

ABSTRACT

With respect to a newly developed titanium alloy Ti–6Al–4V–4Zr–Mo (Ti6441), electric pulse heat (EPH) treatment is innovatively employed to modulate lamellar microstructure details. It is interesting to find that, without mechanical processing such as forging, the EPH treatment can significantly decrease the prior beta grains size down to 390 μm from its original size of 520 μm. Further microstructure analyses show that alpha colonies, as well as alpha plates, are also refined correspondingly. The refinement behaviors are contributed by the unique effects of electric pulses, such as the acceleration of nucleation rate and the retard of grain growth. Especially, the EPH treatment has the orientation of alpha colonies tailored to be regularly 60°-intersected, different from the irregularly oriented lamellar structure treated by conventional heat-treatment furnace. Dynamic compression test results show that the fracture strain of the EPH-treated specimen is obviously increased from 23% to 29%, owing to the attenuation of local stress concentration, and the fracture strength retains a fairly high level. According to the forced shearing experiment results, the susceptibility to the adiabatic shear bands (ASBs) of the Ti6441 alloy after the EPH treatment is declined, because of the apparent ASBs' deflection and bifurcation.

© 2011 Elsevier B.V. All rights reserved.

1. Introduction

Titanium and titanium alloys are widely used for military purposes, e.g. recent applications for armor materials of combat vehicles, due to their excellent properties such as low density and high specific strength [1–3]. One of the most important aspects on the investigation of titanium alloys is microstructure characteristics, because the mechanical properties of these alloys are strongly dependent on their microstructures, which are mainly divided into lamellar, bimodal and equiaxed ones according to heat treatment and thermo mechanical processing [4,5]. Among them, the lamellar microstructure is known to have preferable specific strength, fracture toughness, creep resistance and resistance to crack propagation, but lower ductility, due to the fact that the lamellar microstructure has relatively larger prior beta grains size [6–8]. Therefore, in order to obtain desired mechanical properties, the detailed microstructure parameters, such as prior beta grains size, alpha colonies size and thickness of alpha plates, of

titanium alloys with lamellar microstructures, and the relationship between microstructure characteristics and mechanical properties have been extensively studied. Lee et al. [9] investigated the effects of lamellar microstructure parameters on the dynamic torsional deformation behaviors of Ti–6Al–4V alloys. They reported that the possibility of adiabatic shear bands (ASBs) formation in the microstructure with alpha colonies and alpha plates both in large size was the highest. Besides, Lütjering [6] and Bhattacharjee et al. [10] pointed that the decrease in the thickness of alpha plates generally resulted in an increase in the yield stress and quasi-static tensile ductility. Besides, the size of prior beta grains is an important parameter of lamellar microstructure characteristics. Many researchers [11–13] have focused on determining the prior beta grains size and mechanical property relationships. They claimed that the coarse grain caused negative effects on yield strength and ductility. However, the large prior beta grains size could not be avoided merely by heat treatment using a conventional furnace [13].

Recently, electric pulse heat (EPH) treatment is known as an effective method to improve the properties of metallic materials, and one of the most interesting research results points out that, with rapid heating and subsequent fast cooling methods during EPH treatment process, small grains can be obtained [14–17]. Valeev and Kamalov [14] studied the features of structure formation and

* Corresponding author at: School of Materials Science and Engineering, Beijing Institute of Technology, Beijing 100081, China. Tel.: +86 010 68911144; fax: +86 010 68911144x869.

E-mail address: fanqunbo@bit.edu.cn (Q. Fan).

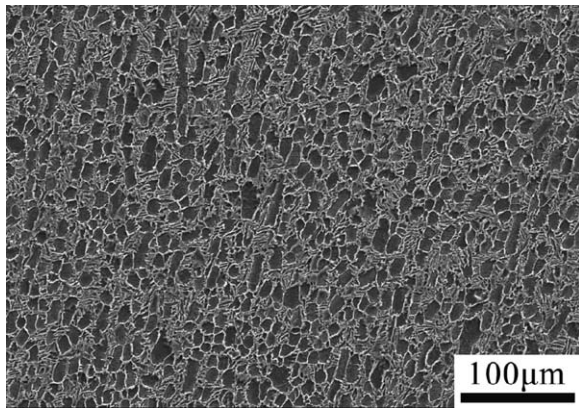


Fig. 1. SEM micrographs of the Ti6441 alloys in as-received state.

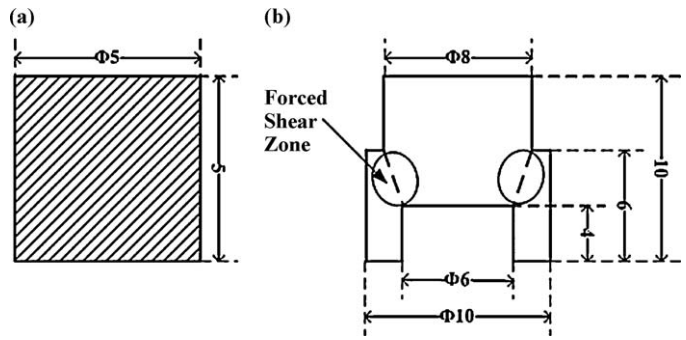


Fig. 2. Geometrical shape and size of the (a) cylindrical specimens and (b) hat specimens for dynamic mechanical properties tests and forced shear tests, respectively (unit: mm).

changes in micro hardness of pre-deformed copper. They concluded that the action of electric pulses lead to grain refinement and thus resulted in the increase of micro hardness. Unfortunately, little information has been reported for utilizing electric pulse heat treatment to vary the detailed microstructure characteristics of titanium alloys with lamellar microstructures.

The objective of the present work, therefore, is to modulate the lamellar microstructure details of titanium alloy by using EPH treatment, thus improving its dynamic mechanical properties. The material used in this study is Ti–6Al–4V–4Zr–Mo (Ti6441), a newly developed titanium alloy at Beijing Institute of Technology. Effects of microstructure characteristics (before and after EPH treatment) on dynamic compression and forced shearing behaviors are investigated.

2. Materials and methods

The beta-transus temperature of Ti6441 alloy was determined at 945 °C. The typical microstructure of the alloy in as-received state was consisted of equiaxed grains with uniform size, as shown in Fig. 1, which was produced via alpha + beta processing route, i.e. initial forging in the beta phase region and final forging in the alpha + beta phase region.

As shown in Table 1, starting from the globular as-received state, the Ti6441 alloys were heat treated in a conventional heat-treatment furnace above the beta-transus temperature (at 960 °C) for 1 h, followed by air cooling to obtain typical lamellar microstructures, named L0. Then, the EPH treatment was performed on the L0 microstructure by heating to 1020 °C at a high temperature rising rate of 100 °C/min, then soaking for 10 min, followed by air cooling to room temperature to obtain a new lamellar microstructure, named LP. The metallographic analyses were made by optical microscopy (OM), scanning electron microscopy (SEM) and transmission electron microscopy (TEM). In order to facilitate distinguishing the primary alpha and beta phases in the SEM micrographs, Image-Pro Plus 6.0 was used to improve the image contrast. Both the average size of prior beta grains and alpha plates were calculated by using the Image-Pro Plus 6.0.

The dynamic compression tests and forced shearing tests were performed by a Split Hopkinson Pressure Bar (SHPB) system. The geometrical shape and size of specimens were shown in Fig. 2.

Table 1
Heat treatment parameters for the Ti6441 alloys.

Specimens no.	Heat treatment
L0	960 °C/1 h/AC
LP	960 °C/1 h/AC + EPH 1020 °C/10 min/AC

Dynamic compression tests were conducted on cylindrical specimens with a diameter of 5 mm and a height of 5 mm, as illustrated in Fig. 2 (a). By data acquisition system, the original pulses of incident, reflected and transmitted waves were recorded. Then, true dynamic compress stress–strain curves at a high strain rate condition were obtained by calculating the stress, strain and strain rate from the original pulses. To investigate the dynamic deformation behaviors of Ti6441 alloys, the critical fracture strain, i.e. the finishing point of uniform plastic deformation, was defined when the flow stress fell to 90% of the maximum stress and indicated by arrows in the dynamic stress–strain curves. The fracture surfaces of the specimens after dynamic compression tests were observed using the SEM. Forced shearing tests were carried out on hat-shaped specimens (Fig. 2(b)) with a height of 10 mm and a maximum diameter of 10 mm. Due to the specimen's special hat-like shape, the adiabatic shear deformation was forced to occur in a narrow region. By data acquisition, a voltage–time curve at a certain strain rate was obtained and the voltage value was proportional to the applied load. The curves recorded the entire response time of the samples, from the very initial stage when subject to the dynamic load to the formation of ASBs, followed by final fracture. If the specimens underwent adiabatic shear failure, the bearing time would be $\leq 80 \mu\text{s}$ (the loading time of incident pulses in the current work). Thus, the susceptibility to the ASBs of specimens with different lamellar characteristic parameters before and after the EPH treatment could be characterized using the voltage–time curves at a certain strain rate. The ASBs within the specimens were further examined by SEM and TEM.

3. Results and discussion

3.1. Microstructures before and after EPH treatment

3.1.1. Prior beta grains

The L0 and LP microstructures of the Ti6441 alloys observed by the OM are shown in Fig. 3(a) and (b), respectively. It can be seen from Fig. 3(a) that the typical beta-annealed lamellar microstructure, L0, is composed of thin lath-type alpha and beta plates, and the coarse-grained lamellar microstructure is divided into colonies of lamellae packages with different orientation angles. As calculated by the Image-Pro Plus 6.0, the coarse-grained L0 microstructure has an average prior beta grains size of 520 μm . In contrast, significant refinement is induced under EPH treatment, as shown in Fig. 3(b). After EPH treatment, the LP microstructure consists of smaller prior beta grains with an average size of 390 μm .

Metallographic analysis reveals that lamellar microstructure of Ti6441 alloy undergoing a subsequent EPH treatment performs refinement behavior and it is amazing that the present refinement of prior beta grains is achieved merely by EPH treatment,

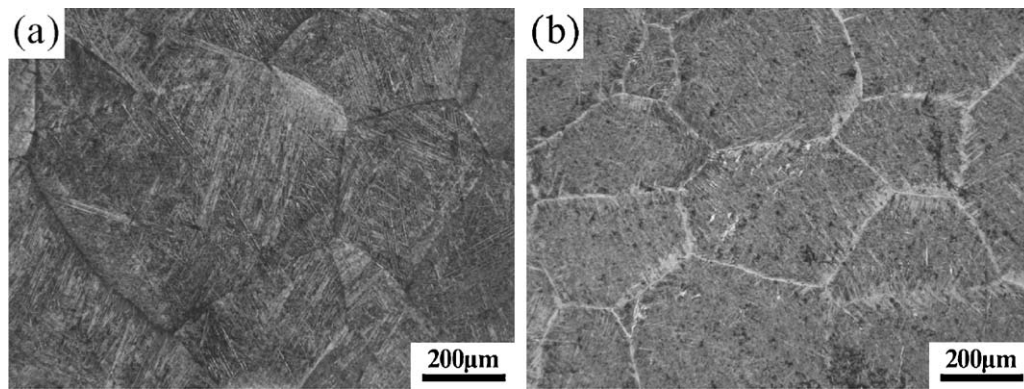


Fig. 3. OM micrographs of the lamellar (a) L0 and (b) LP microstructures, before and after EPH treatment, respectively.

not involving mechanical processing such as forging. This phenomenon, which is similar to the action that electric pulses lead to grain refinement of amorphous alloys and cold worked metals (Cu, Al), rarely occurs in titanium alloys. Though the effect of EPH treatment on refinement of metallic materials is complex, previous literatures [18–20] reported that along with the enhancement of the nucleation rate, there occurred a reduction in the initial crystallized grain size, as well as the retardation in the subsequent rate of grain growth. Therefore, considering the alpha phases within L0 microstructure will be converted into beta phases during the warming up and holding process of the EPH treatment, electric pulses, accelerating nucleation, make the nuclei sites increased during the subsequent cooling process where the diffusion-controlled phase transformation from beta phases to alpha phases is occurred, resulting in the augment of grain boundary alpha phases. Thus, prior beta grains within LP microstructure show a smaller size in contrast with L0 microstructure.

3.1.2. Alpha colonies and alpha plates

To clearly exemplify the influence of the EPH treatment on the detailed lamellar microstructure characteristics of the Ti6441 alloys, the observations on alpha colonies within a prior beta grain are performed by the SEM and the TEM, respectively. The SEM micrographs of the L0 and LP microstructures are shown in Fig. 4(a) and (b), respectively. Fig. 4(c) and (d) are local magnified SEM micrographs of the center regions of the prior beta grains, which show the microstructure details of alpha plates more clearly. As presented in Fig. 4(a) and (c), in the L0 microstructure without undergoing EPH treatment, nuclei of alpha phases form preferentially at the prior beta grain boundaries and the alpha phases grow fast into the grain interior from the grain boundaries along certain atomic planes. As a result, an alpha colony is developed. At the same time, nucleation occurs at the inside of the prior beta grain and then alpha colonies with different orientation are produced. Therefore, the L0 microstructure has an irregularly oriented lamellar

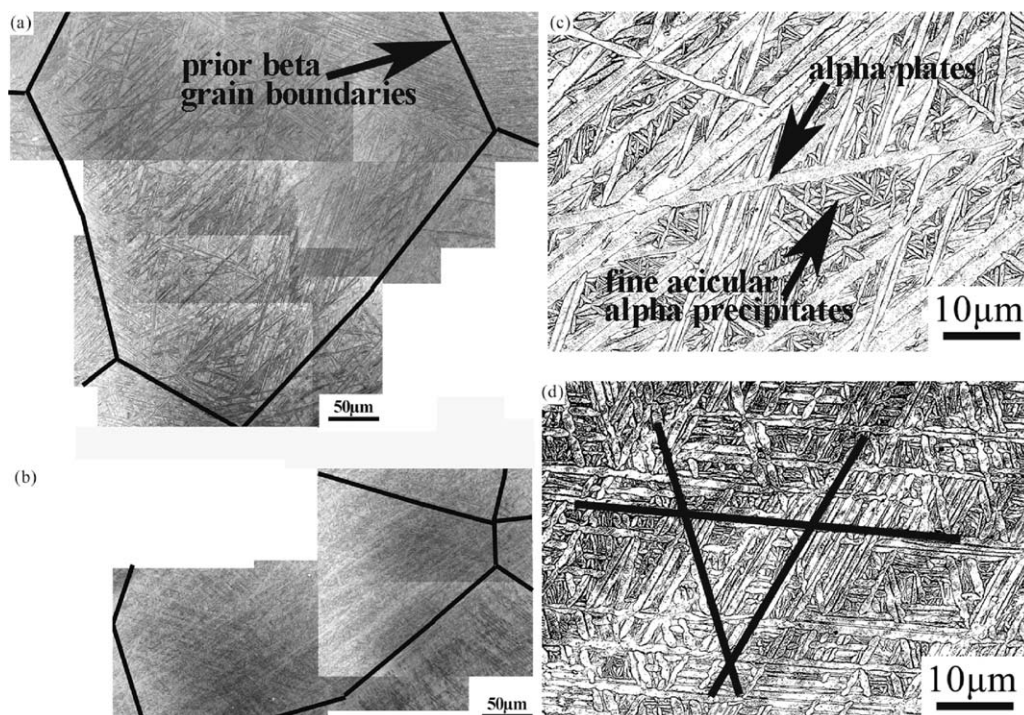


Fig. 4. SEM micrographs of the lamellar (a), (c) L0 and (b), (d) LP microstructures, before and after EPH treatment, respectively. (c), (d) are the magnified images of partial region within (a) and (b), respectively.

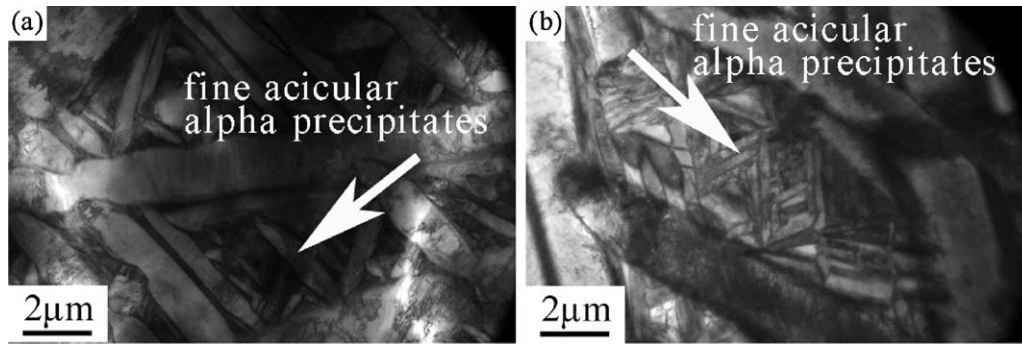


Fig. 5. TEM micrographs of the lamellar (a) L0 and (b) LP microstructures before and after EPH treatment, respectively.

structure, with average alpha plates size of $1.64\ \mu\text{m}$, which is clearly illustrated in Fig. 4(c). In contrast with L0 microstructure, however, as one can see from Fig. 4(b) and (d), alpha colonies within LP are mainly regularly intersected in three directions along the black line as shown in Fig. 4(d), about 60° between each other. Apparently, the EPH treatment can tailor the orientation of alpha colonies, though further studies in future need to be done to verify whether the transient electric pulse or rapid temperature rising is the underlying reason. As calculated by the Image-Pro Plus 6.0, the average size of alpha plates within LP microstructure is about $0.93\ \mu\text{m}$, much thinner than that within L0. TEM studies of the fine acicular alpha precipitates within beta matrix, which exist at the intersection regions of lamellae colonies with different orientations, are shown in Fig. 5. As a result of the EPH treatment, the LP microstructure exhibits much thinner size and more sufficient quantity of acicular alpha precipitates, in contrast with L0 microstructures.

In comparison to the lamellar microstructure obtained at the conventional heat-treatment furnace, the size of alpha colonies, alpha plates within the alpha colony and fine acicular alpha precipitates within beta matrix all decreases after the EPH treatment. Realizing that the EPH treatment has the grain growth of alpha plates retarded, the alpha plates transforming from beta phases are prevented to grow, thus LP microstructure exhibiting a thinner size of alpha colonies and alpha plates. Correspondingly, the LP microstructure with fewer beta matrix vol.%, resulting from relatively higher nucleation rate of alpha plates, cannot offer enough room for the fine acicular alpha precipitates to grow. Thus, the LP microstructure exhibits much thinner size of acicular alpha precipitates in contrast with the L0 microstructures.

3.2. Dynamic compression deformation behaviors before and after EPH treatment

Fig. 6 shows true stress–strain curves of the Ti6441 alloys with L0 and LP microstructures respectively at the strain rate of $3600\ \text{s}^{-1}$, and the arrows in the curves indicate the critical fracture strain and the corresponding stress points. It can be seen that the flow stress of the two microstructures shows a similar varied tendency as the strain increases. The maximum stress point is reached immediately after little plastic deformation, and after that point the flow stress roughly retains a certain value with increasing the strain due to the balance of strain hardening, strain rate hardening and thermal softening, presenting a low level of strain hardening. As the strain proceeds to increase, thermal softening, which is overriding strain rate hardening and strain hardening, is sufficient to induce plastic instability and stress decreases sharply, resulting in the final adiabatic shear failure.

It can be seen from Fig. 6 that the LP microstructure has nearly the same level of dynamic strength with the L0 microstructure. The strength of the LP microstructure can be controlled by beta

grain size, volume fraction of phases and solid solution of elements. On the one hand, the effect of beta grain size on the strength can be estimated by the Hall-Perch relation, and the strength of LP microstructure presents an increasing trend due to the grain refinement. On the other hand, resulting from relatively higher nucleation rate of alpha plates during EPH treatment, the LP microstructure with a fewer volume fraction of beta phases, which have higher strength than alpha phases, has a trend to show a lower strength in contrast with the L0 microstructure. Besides, the contribution of solution strengthening is inferred to be declined after EPH treatment and the corresponding findings will be discussed in a future article. The above three aspects are in competition with each other and the comprehensive result shows that the strength of LP microstructure does not significantly change in contrast with the L0 microstructure.

As shown in Fig. 6, although the dynamic strength retains nearly the same high level, the LP microstructure undergoing EPH treatment performs much outstanding dynamic ductility with 29% in the fracture strain, in contrast with the L0 microstructure having the fracture strain of 23%, at the $3600\ \text{s}^{-1}$ strain rate. This means that at the same strain rate, the LP microstructure can absorb much more energy due to the augment of fracture strain during the dynamic compression deformation process, showing the increase of load bearing time in contrast with L0 microstructure. As prior beta grains, alpha colonies, alpha plates and fine acicular alpha precipitates are refined, the significant increase of alpha/beta phase interfaces in LP lamellar microstructures has an advantageous effect on avoiding the stress concentration at the boundary

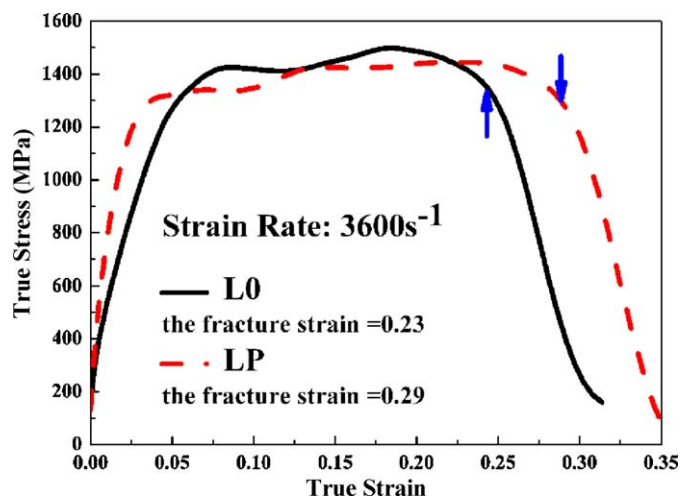


Fig. 6. Stress–strain curves obtained from the dynamic compression test. The arrows indicate the critical fracture strain and the corresponding stress points of Ti6441 alloys with L0 and LP microstructures, respectively.

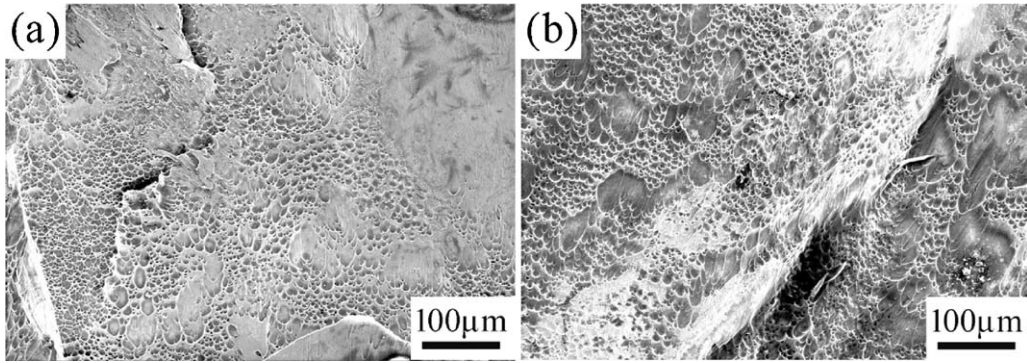


Fig. 7. SEM fractographs of the dynamically fractured specimens for the (a) L0 and (b) LP microstructures, respectively.

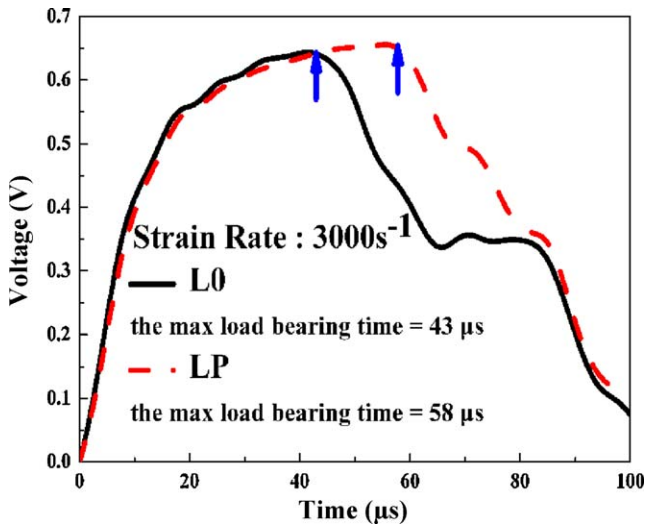


Fig. 8. Voltage–time curves for the forced shearing specimens under the same strain rate. The arrows indicate the maximum load bearing time points of Ti6441 alloys with L0 and LP microstructures, respectively.

of alpha/beta phase, because each alpha/beta interface is assigned to less stress. Hence, the LP microstructure can bear much longer time before fracture failure than the L0 one at the strain rate of 3600 s⁻¹, showing the better dynamic ductility.

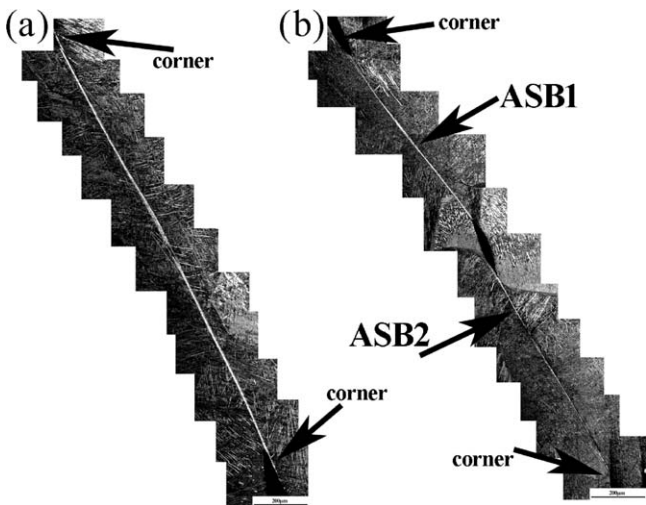


Fig. 9. OM micrographs of ASBs within (a) L0 and (b) LP microstructures of Ti6441 hat-shaped specimens.

SEM fractographs of Ti6441 cylindrical specimens with L0 and LP microstructures after dynamic compression tests are shown in Fig. 7(a) and (b), respectively. As presented in Fig. 7, the fractured compressed specimens for both the L0 and LP microstructures show a typical adiabatic shear fracture mode [21], composed of smooth shear regions and ductile dimples. However, it can be induced from the SEM fractographs that the LP microstructure shows higher dynamic ductility than the L0 one, because the area of ductile dimples regions and the size of dimples increase with the EPH treatment appointed.

3.3. Susceptibility to adiabatic shear bands before and after EPH treatment

Fig. 8 presents dynamic shear voltage–time curves of the Ti6441 hat-shaped specimens at the strain rate of 3000 s⁻¹, and the arrows

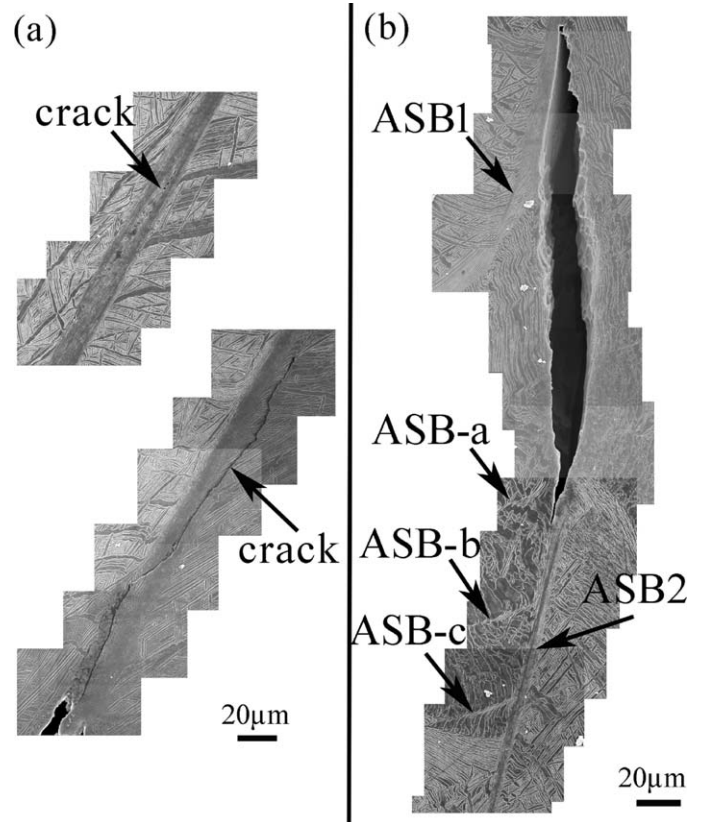


Fig. 10. SEM micrographs of ASBs within (a) L0 and (b) LP microstructures of Ti6441 hat-shaped specimens.

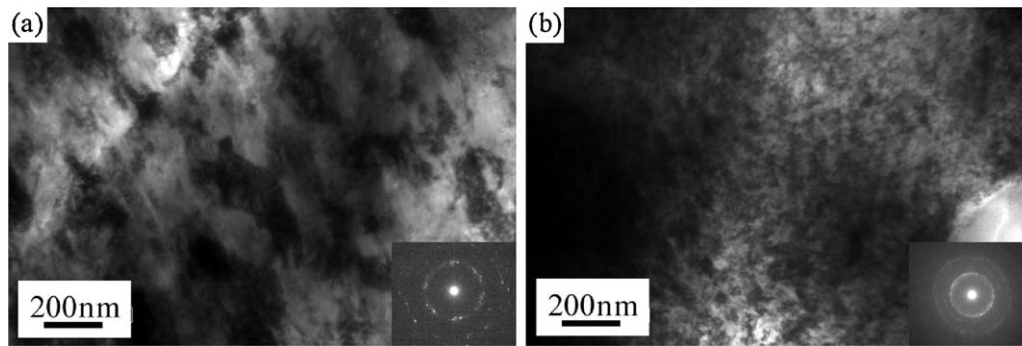


Fig. 11. TEM micrographs and SAD patterns of the center of ASBs within (a) L0 and (b) LP microstructures.

in the curves indicate the maximum load bearing time points of Ti6441 alloys with L0 and LP microstructures, respectively. As it can be seen in Fig. 8, the LP lamellar microstructure can bear 58 μs , which is much longer than the L0 one at a load bearing time of 43 μs , indicating the susceptibility to the ASBs declines after EPH treatment, well agreeing with the aforementioned dynamic compression analysis.

ASBs, characterized by OM and SEM as shown in Figs. 9 and 10, respectively, are generated both in L0 and LP microstructures at the strain rate of 3000 s^{-1} . However, the ASBs feature is different before and after EPH treatment. It can be seen from Fig. 9(a) that the two ASBs within L0 microstructure initiate at every corner of the hat-shaped specimen, where geometrical imperfection causes the strain concentration, and expand very rapidly into the inside of hat-shaped specimen along the maximum shear stress direction until merge into one fully developed shear band, stretching out from one corner to the other corner. Because of the mingled and amalgamated behavior, the ASBs within L0 microstructure seem to be wider than that within LP microstructure. In contrast to the well-defined coherent ASBs within the L0 microstructure, however, the ASBs initiated at every corner of the LP specimen shown in Fig. 9(b), linked by a crack during the second load process, do not intersect into each other but propagate in their own paths, because ASBs undergo much severer deflection at the colonies of the lamellae packages during the development process, resulting from the decrease of alpha colonies and alpha plates size after EPH treatment. The results indicate the LP microstructure can bear more time and exhibit lower susceptibility to adiabatic shear deformation than L0, at the strain rate of 3000 s^{-1} . SEM studies of the ASBs within L0 microstructure show that cracks have already initiated and propagated along the ASBs (Fig. 10(a)). However, it can be seen from Fig. 10(b) that cracks do not exist in the two main ASBs (ASB1 and ASB2) within LP microstructure. In addition, in LP microstructure, three sub-ASBs (ASB-a, ASB-b and ASB-c) shown in Fig. 10(b) at the arrows are observed, illustrating the phenomenon of ASBs bifurcation. In brief, ASBs analyses reveal that comparing to the L0 microstructure, the LP microstructure with thinner alpha colonies and alpha plates after EPH treatment much severely hinders the ASBs growth, inducing the ASBs strongly deflects at the boundary of alpha colonies, correspondingly causing the bifurcation of ASBs and the increase of ASBs propagation path. The combined effect of bifurcation formatting and ASBs length increasing requires much more energy by consuming metal bulk plastic deformation work, accordingly reducing the possibility of cracks formation within ASBs followed by fracture failure. Hence, the LP microstructure, which can bear a longer time during the dynamic load process in contrast with the L0 one at 3000 s^{-1} , performs lower susceptibility to ASBs.

The magnified micrographs in the center of the ASBs within L0 and LP microstructures are illustrated by TEM, as shown in

Fig. 11(a) and (b), respectively. TEM observations reveal that both microstructures undergo a dynamic recrystallization in the shear band core region. However, the extent of dynamic recrystallization shows a distinction between L0 and LP microstructures. From Fig. 11(a), in the L0 microstructure, it can be seen that equiaxed recrystallization grains with diameters of about 200 nm exist in the center of ASBs, and the selected area diffraction (SAD) pattern taken from this area shows that discrete circles are formed (the inset in Fig. 11(a)), demonstrating the lower extent of dynamic recrystallization. However, the dynamic strain of LP microstructure is larger in contrast with L0 microstructure at the same strain rate, which accounts for the augment of load bearing time before fracture failure, illustrating the extent of dynamic recrystallization in the center of the ASBs within LP microstructure becomes severer. Thus, the abundance of extremely fine equiaxed recrystallization grains with a size of 50 nm exist in ASB center area are produced, as shown in Fig. 11(b), and the continuous diffraction rings are induced in the SAD pattern (the inset in Fig. 11(b)).

4. Conclusion

In the present study, the effects of EPH treatment on the detailed lamellar microstructure characteristic parameters and dynamic deformation behaviors of a newly developed Ti6441 alloy are investigated. The major results are as follows:

- (1) Different from the conventional furnace heat treatment, prior beta grains within lamellar microstructures after EPH treatment are significantly refined. The size of alpha colonies, alpha plates within the alpha colony and fine acicular alpha precipitates within beta matrix all decrease after EPH treatment. EPH treatment makes the orientation of alpha colonies regularly intersected in three directions with 60° between each other.
- (2) After undergoing EPH treatment, the dynamic ductility of lamellar microstructures is obviously enhanced, while a fairly high level of dynamic strength is retained. Comparing with the lamellar microstructures obtained by conventional furnace heat treatment, the area of ductile dimples regions within the dynamic fracture surface is wider and the size of ductile dimples is larger for the EPH-treated lamellar microstructure.
- (3) The susceptibility to the ASBs of the Ti6441 alloy with EPH-treated lamellar microstructures is declined comparing to the alloy subjected to conventional furnace heat treatment. In the EPH-treated lamellar microstructures, the ASBs deflect severely inducing the formation of ASBs bifurcation, and much severe dynamic recrystallization with continuous diffraction rings occurs in the ASBs core.

Acknowledgements

The SEM research was supported by the Beijing Center for Physical and Chemical Analysis. The TEM research was supported by the School of Physics, Peking University.

References

- [1] S.L. Semiatin, T.R. Bieler, *Metall. Mater. Trans. A* 32 (2001) 1787–1799.
- [2] K. Suzuki, S. Watakabe, *Met. Mater. Int.* 9 (2003) 359.
- [3] B.K. Kad, S.E. Schoenfeld, M.S. Burkins, *Mater. Sci. Eng. A* 322 (2002) 241–251.
- [4] K. Suzuki, M. Yao, *Met. Mater. Int.* 10 (2004) 33.
- [5] D.G. Lee, Y.H. Lee, S. Lee, C.S. Lee, S.M. Hur, *Metall. Mater. Trans. A* 35 (2004) 3103–3112.
- [6] G. Lütjering, *Mater. Sci. Eng. A* 263 (1999) 117–126.
- [7] M. Broun, G. Shakhonova, *Mater. Sci. Eng. A* 243 (1998) 77–81.
- [8] W. Lee, C. Lin, *Mater. Sci. Eng.* 241 (1998) 48–59.
- [9] D.G. Lee, S. Lee, C.S. Lee, S.M. Hur, *Metall. Mater. Trans. A* 34 (2003) 2541–2548.
- [10] A. Bhattacharjee, V.A. Joshi, A.K. Gogia, in: *Titanium '99*, *Sci. Technol.* (1999) 529–535.
- [11] H.M. Flower, *Mater. Sci. Technol.* 6 (1990) 1082–1092.
- [12] G. Lütjering, J. Albrecht, O.M. Ivasishin, *Miner. Met. Mater.* (1994) 65–74.
- [13] C. Sauer, G. Lütjering, in: *Titanium '99*, *Sci. Technol.* (1999) 390–397.
- [14] I.Sh. Valeev, Z.G. Kamalov, *J. Mater. Eng. Perform.* 12 (2003) 272–278.
- [15] Z. Xu, G. Tang, F. Ding, S. Tian, H. Tian, *Appl. Phys. A* 88 (2007) 429–433.
- [16] H. Conrad, *Mater. Sci. Eng.* 287 (2000) 4.
- [17] H. Conrad, *Mater. Trans.* 46 (2005) 1083–1087.
- [18] H. Conrad, *Mater. Sci. Eng. A* 287 (2000) 227–237.
- [19] H. Conrad, N. Karam, S. Mannan, A.F. Sprecher, *Scripta Metall.* 22 (1988) 235–238.
- [20] H. Conrad, Z. Guo, A.F. Spreche, *Scripta Metall.* 23 (1989) 821–823.
- [21] X.Q. Liu, C.W. Tan, J. Zhang, Y.G. Hu, H.L. Ma, F.C. Wang, H.N. Cai, *Mater. Sci. Eng. A* 501 (2009) 30–36.